Indian Journal of Pure & Applied Physics
Vol. 58, May 2020, pp. 336-341

Evaporation residue cross section to synthesize superheavy element Z=119

H C Manjunatha[a*], K N Sridhar[b] & N Sowmya[a]

[a]Department of Physics, Government College for Women, Kolar 563 101, India
[b]Department of Physics, Government First Grade College, Kolar 563 101, India

Received 23 March 2020

The evaporation-residue cross section σ_{EVR} of fusion reactions depend on the projectile-target combinations and the incident energy. A detail theoretical study is useful before the synthesis of more isotopes of super heavy nuclei Z=119. We have studied the evaporation-residue cross sections for possible projectile-target combinations to synthesis the superheavy nuclei with Z=119. We have studied the dependence of evaporation residue cross section with that of mass number of the target, product of atomic numbers of projectile and target (Z_1Z_2), fusion barrier height (V_b) and fusion barrier width (R_b). After the detailed analysis, we have identified the most probable projectile-target combinations. The identified projectile-target combinations to synthesis superheavy nuclei $^{295\text{-}296}119$ are $^{45}Sc+^{250,251}Cf$. We hope that our predictions guide the future experiments in the synthesis of super heavy nuclei $^{295\text{-}296}119$.

Keywords: Superheavy nuclei, Evaporation residue, Fusion barrier

1 Introduction

There has been much experimental progress in synthesizing superheavy elements. The island of stability was predicted theoretically four decades before. In the previous decade, existence of island of stability has been experimentally confirmed[1,2]. For the synthesis of element 119, Adamian *et al.,*[3] studied the hot fusion reactions $^{50}Ti+^{247-249}Bk$ and $^{51}V+^{246-248}Cm$. Superheavy nuclei with Z=112–118 were successfully synthesised using fusion reactions with ^{48}Ca beam and various actinide targets at FLNR (Dubna), GSI (Darmstadt), and LBNL (Berkeley)[4–12]. Previous researchers attempted[13-15] to synthesize the nuclei Z=119 and 120. The production cross sections of superheavy elements using hot fusion reactions for the synthesis of Z=119 and 120 were evaluated by Zhu *et al.*,[16]. Liu and Bao[17] using hot fusion reaction of $^{50}Ti+^{249}Bk$ evaluated evaporation residue cross sections for the synthesis of the superheavy element Z=119. Wang *et al.*,[18] evaluated the physical parameters for the synthesis of superheavy nuclei with Z=119 and 120 in heavy-ion reactions with trans-uranium targets. Lougheed *et al.*,[19] using the reaction $^{48}Ca+^{254}Es$, was the first to attempt for the synthesis of superheavy element Z=119. Hot-fusion reactions with ^{50}Ti as the projectile were studied using the di-nuclear system model[20,21].

The evaporation-residue cross section σ_{EVR} of fusion reactions depends on the projectile-target combination and the incident energy. Therefore, finding favourable reactions and the optimal beam energy range are very important for the synthesis of superheavy elements. In the previous work, we have also studied the possible projectile target combinations for the synthesis of superheavy nuclei and competition between different decay modes of super heavy nuclei[22-35].

A detail theoretical study is useful before the synthesis of super heavy nuclei $^{295\text{-}296}119$. Hence in the present work, we have identified the most probable projectile-target combination by studying the fusion cross section, evaporation residue cross section, compound nucleus formation probability (P_{CN}) and survival probability (P_{Surv}) of different projectile target combinations for the synthesis of super heavy element Z=119.

2 Theoretical Frame Work

2.1 Fusion cross section

The interacting potential between two nuclei of fusion fragments is taken as:

$$V = \frac{Z_1 Z_2 e^2}{r} + V_p(z) + \frac{\hbar^2 l(l+1)}{2\mu r^2} \quad \ldots (1)$$

Here Z_1 and Z_2 are the atomic numbers of projectile and target and r is the distance between centres of the

*Corresponding author (E-mail: manjunathhc@rediffmail.com)

projectile and target. The second term V_p (z) is the proximity potential. In the third term l represents the angular momentum, and μ the reduced mass.

The proximity potential (V_P) given by Blocki *et al.* [36] as:

$$V_p(z) = 4\pi\gamma b\left[\frac{C_1C_2}{C_1+C_2}\right]\Phi(\xi) \quad \ldots (2)$$

where the nuclear surface tension coefficient is given by:

$$\gamma = 0.9517[1-1.7826(N-Z)^2/A^2]\ \text{MeV/fm}^2 \quad \ldots (3)$$

here N, Z, and A are the neutron, proton, and mass number of the parent and Φ represents the proximity function. Myers and Swiatecki [37] modified the proximity potential using the concepts of droplet model, nuclear radii and surface tension coefficients. Using the droplet model, matter radius C_i was calculated as:

$$C_i = R_i + \frac{N_i}{A_i}t_i \quad \ldots (4)$$

$$\text{Where} \quad R_i(\alpha_i) = R_{0i}\left[1+\sum_\lambda \beta_{\lambda i}Y_\lambda^{(0)}(\alpha_i)\right] \quad \ldots (5)$$

Here α_i is the angle between the radius vector and symmetry axis of i^{th} nuclei and the quadrupole interaction term proportional to $\beta_{21}\beta_{22}$ is neglected because of its short range character. For this potential, R_{0i} denotes the half-density radii of the charge distribution and t_i is the neutron skin of the nucleus. The nuclear charge is given by the relation:

$$R_{00i} = 1.24A_i^{1/3}\left(1+\frac{1.646}{A_i}-0.191\frac{A_i-2Z_i}{A_i}\right)fm \quad \ldots (6)$$

where i = 1, 2. The half-density radius ci was obtained from the relation:

$$R_{0i} = R_{00i}+\left(1-\frac{7}{2}\frac{b^2}{R_{00i}^2}-\frac{49}{8}\frac{b^4}{R_{00i}^4}+.....\right) \quad \text{(i=1, 2)} \quad \ldots (7)$$

Using the droplet model, neutron skin t_i reads as:

$$t_i = \frac{3}{2}r_0\left(\frac{JI_i-\frac{1}{12}c_1Z_iA_i^{-1/3}}{Q+\frac{9}{4}JA_i^{-1/3}}\right) \quad \text{(i=1, 2)} \quad \ldots (8)$$

here r_0 is 1.14 fm, the value of the nuclear symmetric energy coefficient J = 32.65 MeV, $I_i=(N_i-A_i)/Z_i$ and $c_1 = 3e^2/5r_0$ = 0.757895 MeV. The neutron skin stiffness coefficient Q was taken to be 35.4MeV. The nuclear surface energy coefficient γ in terms of neutron skin,

$$\gamma = \frac{1}{4\pi r_0^2}\left[18.63(MeV)-Q\frac{t_1^2+t_2^2}{2r_0^2}\right] \quad \ldots (9)$$

where t_1 and t_2 were calculated using above equation. The universal function for this is given by:

$$\Phi(\xi) = -0.1353+\sum_{n=0}^{5}\frac{c_n}{(n+1)}(2.5-\xi)^{n+1}, \text{ for } 0\le\xi\le 2.5 \quad \ldots (10)$$

$$\Phi(\xi) = -\exp[(2.75-\xi)/0.7176], \text{ for } \xi\ge 2.5 \quad \ldots (11)$$

where $\xi = R - C_1 - C_2$. The values of different constants c_n were c_0 =−0.1886, c_1 = −0.2628, c_2 =−0.15216, c_3 =−0.04562, c_4 =0.069136, and c_5 = −0.011454.

Since fusion happens at a distance larger than the touching configuration of colliding pair, the above form of the Coulomb potential is justified. One can extract the barrier height V_B and barrier position R_B using the following conditions

$$\left.\frac{dV(r)}{dr}\right|_{r=R_B} = 0 \text{ and } \left.\frac{d^2V(r)}{dr^2}\right|_{r=R_B} \le 0 \quad \ldots (12)$$

To study the fusion cross sections, we shall use the model given by Wong[38]. In this formalism, the cross section for complete fusion is given by:

$$\sigma_{fus} = \frac{\pi\hbar^2}{2\mu E}\sum_{l=0}^{l_{\max}}(2l+1)\times T_l(E_{cm})\cdot P_{CN}(E,l) \quad \ldots (13)$$

where $k=\sqrt{2\mu E/\hbar^2}$ and μ is the reduced mass. The centre of mass energy is denoted by E_{cm}. In the above formula, $l_{\max}$ corresponds to the largest partial wave for which a pocket still exists in the interaction potential and T_l (E_{cm}) is the energy-dependent barrier penetration factor and is given by:

$$T_l(E_{cm}) = \left\{1+\exp\left(\frac{2\pi}{\hbar\omega_l}(V_B-E_{cm})\right)\right\}^{-1} \quad \ldots (14)$$

where $\hbar\omega_l$ is the curvature of the inverted parabola. Here P_{CN} is the probability for the compound nucleus (*CN*) formed when two nuclei comes in contact. For specific nuclear combinations leading to so called "cold" synthesis a simple parameterization of $P_{CN}(E,l)$ was proposed by previous researcher[39]

$$P_{CN}(E,l)=\frac{P_{CN}^{0}\left(Z_1,Z_2\right)}{1+\exp\left(\frac{E_B^{*}-E_B^{*}(l)}{\Delta}\right)} \quad \ldots (15)$$

Here E_B^{*} is the excitation energy of compound nucleus at the Bass barrier and $E_B^{*}(l)=E+Q-E_{rot}(l)$, where Q is the fusion Q value, $E_{rot}(l)$ is the rotational energy and it is given by $E_{rot}(l)=\frac{\hbar^2}{2I_{gs}}l(l+1)$ and

$$P_{CN}^{0}=\frac{1}{1+\exp\left(\frac{Z_1Z_2-\varsigma}{\tau}\right)} \quad \ldots (16)$$

where and ς =1760 τ=45.

2.2 Evaporation residue cross section and survival probability

The compound nucleus is formed by nucleon transfer from the light nucleus to the heavy one by overcoming the inner fusion barrier. The cross section of SH element production in a heavy-ion fusion reaction with subsequent emission of *x* neutrons, y protons, and z alphas

$$\sigma_{EVR}=\frac{\pi\hbar^2}{2\mu E}\sum_{l=0}^{l_{\max}}(2l+1)\times T_l(E_{cm})\cdot P_{CN}(E,l)\cdot P_{xn,yp,z\alpha}(E,l) \quad \ldots (17)$$

Then the survival cross section is

$$\sigma_{Surv}=\frac{\pi\hbar^2}{2\mu E}\sum_{l=0}^{l_{\max}}(2l+1)\times T_l(E_{cm})\cdot P_{CN}(E,l)\cdot P_{Surv}(E,l) \quad \ldots (18)$$

Where P_{Surv} (E,l) is survival probability. It is the probability of surviving the compound nucleus against the fission and after the emission of *x* neutrons, y protons, and z alphas. It is given as:

$$P_{Surv}(E,l)=\sum_{x,y,z}P_{xn,yp,z\alpha}(E,l) \quad \ldots (19)$$

It is assumed that the excited nucleus may decay through the emission of light particles (neutrons, protons or alpha particles), emission of gamma rays and by fission into heavy fragments. The expression for calculation of the particle emission widths are given by:

$$\Gamma_{C\to B+b}(E^{*},J)=\frac{2S_b+1}{2\pi\rho_c\left(E^{*},J\right)}\int_0^{E^{*}-B_b}\sum_l T_l\left(e_b\right)\cdot\sum_{I=|J-l|}^{I=|J+l|}\rho_B\left(E^{*}-B_b-e_b,I\right)de_b \quad \ldots (20)$$

Here S_b is the spin of emitted particle and B_b is its binding energy, where b=n, p, α. e_b is the kinetic energy of the emitting particle. Where ρ_C and ρ_b are level densities of the compound nucleus and emitted particle[40]. $T_l(e)$ is the probability that the particle will pass through the potential barrier. For charged particles the probability that the particle will pass through the potential barrier is:

$$T_l(e)=\frac{P(e)}{\left[1+\exp\left[\frac{2\pi}{\hbar\omega}\left(V_c+\frac{\hbar^2l(l+1)}{2\mu R^2}-e\right)\right]\right]} \quad \ldots (21)$$

where $P(e)=\frac{\sqrt[4]{\frac{e}{e+40}}}{\left[1+\sqrt{\frac{e}{e+40}}\right]^2}$, $R=r_0A^{1/3}+2$ fm and μ is the reduced mass of the particle. For neutrons the probability is calculated using the formula:

$$T_l(e)=P(e)\exp\left[-2\sqrt{\frac{2\mu e}{\hbar^2}}\left(\rho^2-R^2+\rho\log\left(\frac{\rho+\sqrt{\rho^2-R^2}}{R}\right)\right)\right]$$

where $\rho=\sqrt{\frac{\hbar^2l(l+1)}{2\mu e}}$ … (22)

The fission width is calculated from the expression:

$$\Gamma_{fiss}(E^{*},J)=\frac{K_{krqmers}}{2\pi\rho_c\left(E^{*},J\right)}\int_0^{E^{*}}\sum_l T_{fiss}\left(e_b,J\right)\cdot\rho_C^{S.P}\left(E^{*}-e,J\right)de \quad \ldots (23)$$

Where $T_{fiss}(e,J)=\frac{1}{\left[1+\exp\left[-\frac{2\pi}{\hbar\omega_{S.p}}\left(e-B\left(E^{*}\right)\right)\right]\right]}$ is the fission barrier penetrability,

$K_{Kramers} = \frac{\hbar\omega_{g.s}}{T\omega_{s.p}}\left(\sqrt{\omega_{S.P}^2 + \frac{\eta^2}{4}} - \frac{\eta}{2}\right)$ is the Kramers factor[41]

η is the viscosity parameter, $\omega_{g.s}$ and $\omega_{s.p}$ are the curvatures of the potential at the ground state and saddle point, respectively. The fission barrier is calculated by the formula:

$$B_{fiss}(U) = B_{LDM} + \delta U\left(1 - \exp(-\gamma U)\right) \quad \ldots (24)$$

where B_{LDM} is the liquid-drop fission barrier[42], δU is the shell correction to the ground state [23]. Subsequent estimation of the total probability for the formation of a cold residual nucleus after the emission of *x* neutrons and N gammas $C \rightarrow B + xn + N\gamma$ is

$$P_{xn} = \int_0^{E_0^* - B_n(1)} \frac{\Gamma_n}{\Gamma_{tot}}(E_0^*, I_0)\cdot W_n(E_0^*, e_1)de_1 \int_0^{E_1^* - B_n(2)} \frac{\Gamma_n}{\Gamma_{tot}}(E_1^*, I_1)\cdot W_n(E_1^*, e_2)de_2 \int_0^{E_1^* - B_n(x)} \frac{\Gamma_n}{\Gamma_{tot}}(E_{x-1}^*, I_{x-1})\cdot W_n(E_{x-1}^*, e_x)\cdot \prod_{i=1}^{N}\frac{\Gamma_\gamma}{\Gamma_{tot}}(E_i^*, I_i)de_x \quad \ldots (25)$$

Here $B_n(x)$ and e_i are the binding and kinetic energies of the i^{th} evaporated neutron, E_i^* is the excitation energy of the residual nucleus after the emission of *i* neutrons. $W_n(E^*e) = C_n\sqrt{e}\exp\left[-e/T(E^*)\right]$ is the probability for the evaporated neutron to have energy *e*, and the normalization coefficient C_n is determined from the condition $\int_0^{E^*-B} W_n(E^*e)de = 1$.

3 Results and Discussion

In the present work, we have studied the variation of evaporation residue cross section as a function of mass number of the targets. Figures 1 and 2 show the variation of evaporation residue cross section for[295-296]119 vs mass number of the targets at different energies and for 1n - 5n reactions. The evaporation residue cross section increases with increase in the mass number of the targets. From the study of Figs 1 and 2, it is found that the projectile-target combinations such as $^{45}Sc + ^{250,251}Cf$ are having the larger cross-sections compared to that of other projectile-target combinations.

Figures 3 and 4 show the variation of evaporation residue cross section for[295-296]119 with the product of atomic numbers of projectile and target nuclei (Z_1Z_2) at different energies and for 1n - 5n reactions. The evaporation residue cross section decreases with

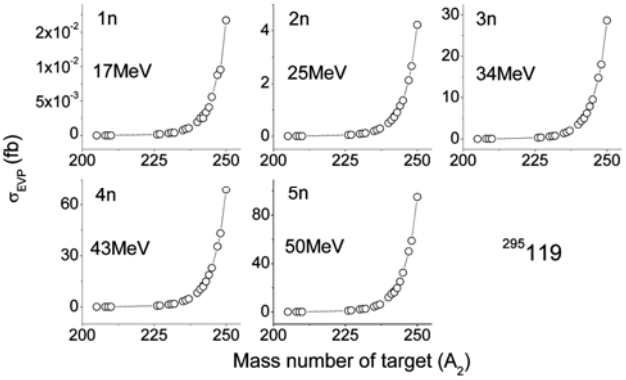

Fig. 1 – Variation of evaporation cross section with mass number of the target for the compound nuclei ^{295}119.

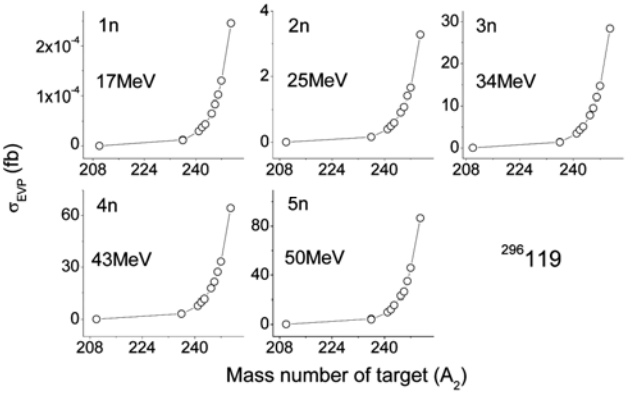

Fig. 2 – Variation of evaporation cross section with mass number of the target for the compound nuclei ^{296}119.

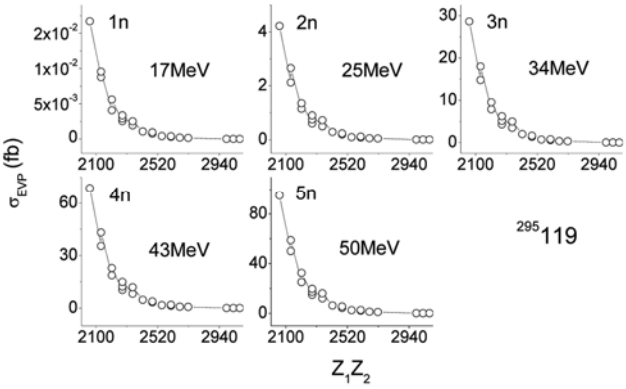

Fig. 3 – Variation of evaporation residue cross section with the product of atomic numbers of projectile and target nuclei (Z_1Z_2) for the compound nuclei ^{295}119.

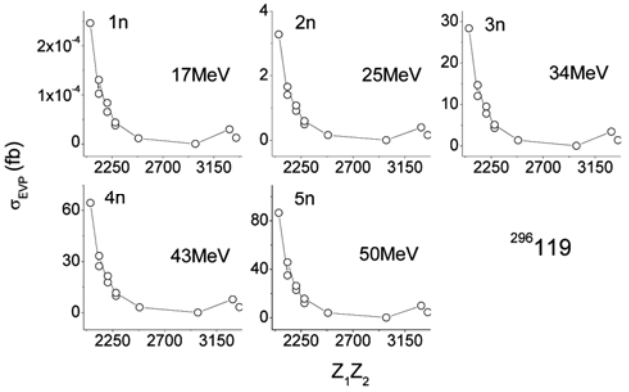

Fig. 4 – Variation of evaporation cross section with the product of atomic numbers of projectile and target nuclei (Z_1Z_2) for the compound nuclei ^{296}119.

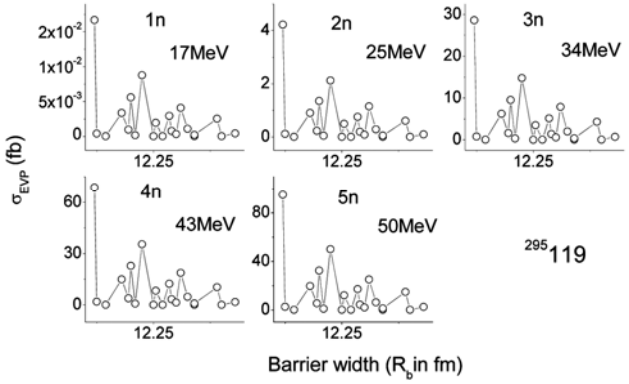

Fig. 5 – Variation of evaporation cross section with barrier position (R_b) for the compound nuclei ^{295}119.

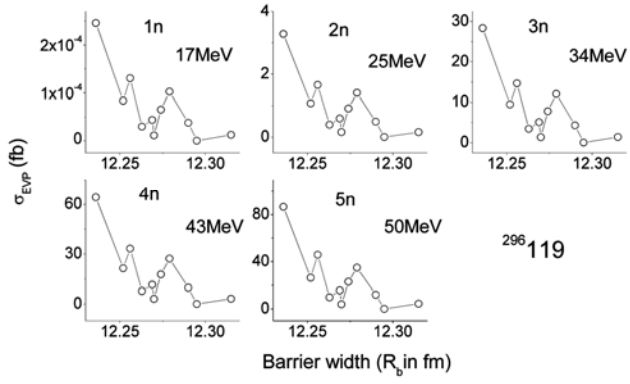

Fig. 6 – Variation of evaporation cross section with barrier position (R_b) for the compound nuclei ^{296}119.

increase in the product of atomic numbers. From the observation of Figs 3 and 4, it is noted that the evaporation residue cross section decreases with increase in Z_1Z_2, due to the increase in the repulsive force between the two fusing nuclei.

Figures 5 and 6 show the variation of evaporation residue cross section for $^{295\text{-}296}$119 versus barrier

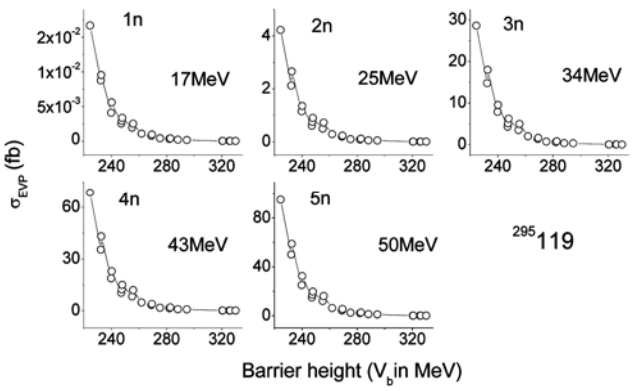

Fig. 7 – Variation of evaporation cross section with barrier height (V_b) for the compound nuclei ^{295}119.

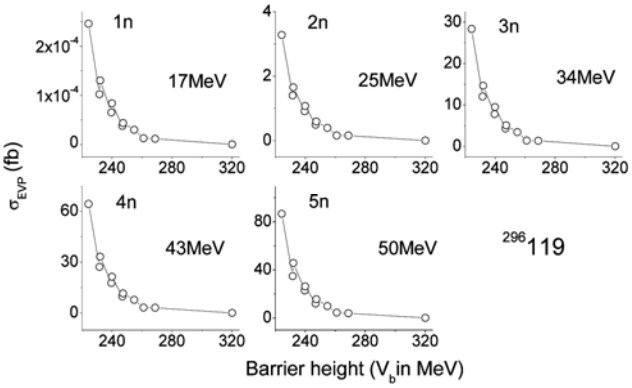

Fig. 8 – Variation of evaporation cross section with barrier height (V_b) for the compound nuclei ^{296}119.

position (R_b) at different energies and for 1n - 5n reactions. The evaporation residue cross section decreases with increase in the barrier position (R_b). From the Figs 5 and 6, it is observed that the evaporation residue cross sections are maximum for the smaller values of fusion barrier positions. Figures 7 and 8 show the variation of evaporation residue cross section for $^{295\text{-}296}$119 versus barrier height (V_b) at different energies and for 1n - 5n reactions. The evaporation residue cross section decreases exponentially with increase in barrier height (V_b). From the detailed analysis, it is found that the projectile-target combinations which are having larger values of the fusion barrier height (V_b) and smaller values of fusion barrier position (R_b) produces maximum evaporation residue cross sections. Thus, the projectile-target combinations ^{45}Sc+^{250,251}Cf is suitable for the synthesis of superheavy nuclei Z=119.

4 Conclusions

The selected most probable projectile-target combinations for the synthesis of superheavy nuclei

$^{295\text{-}296}$119 are ^{45}Sc+^{250,251}Cf. We hope that our predictions may help the future experiments in the synthesis of $^{295\text{-}296}$119.

References

1 Oganessian Y T, *J Phys G Nucl Part Phys*, 34 (2007) R165.
2 Hamilton J H, Hofmann S & Oganessian Y T, *Ann Rev Nucl Part Sci*, 63 (2013) 383.
3 Adamian G G, Antonenko N V & Lenske H, *Nucl Phys A*, 970 (2018) 22.
4 Oganessian Y T, Abdullin F S, Bailey P D, Benker D E & Bennett M E, *Phys Rev Lett*, 104 (2010) 142502.
5 Oganessian Y T, Abdullin F S, Dmitriev S N, Gostic J M & Hamilton J H, *Phys Rev C*, 87 (2013) 014302.
6 Utyonkov V K, Brewer N T, Oganessian Y T, Rykaczewski K P, Abdullin F S & Dmitriev S N, *Phys Rev C*, 92 (2015) 034609.
7 Oganessian Y T & Utyonkov V K, *Nucl Phys A*, 944 (2015) 62.
8 Stavsetra L, Gregorich K E, Dvorak J, Ellison P A, Dragojevic I, Garcia M A & Nitsche H, *Phys Rev Lett*, 103 (2009) 132502.
9 Düllmann C, Schadel M, Yakushev A, Türler A, Eberhardt K, Kratz J V, Ackermann D & Andersson L L, *Phys Rev Lett*, 104 (2010) 252701.
10 Gates J M, Düllmann C E, Schadel M, Yakushev A, Turler A, Eberhardt K & Kratz J V, *Phys Rev C*, 83 (2011) 054618.
11 Hofmann S, Heinz S, Mann R, Maurer J, Khuyagbaatar J, Ackermann D, Antalic S & Barth W, *Eur Phys J A*, 48 (2012) 62.
12 Khuyagbaatar J M, Yakushev A, Düllmann C E, Ackermann D, Andersson L L, Asai M, Block M & Boll R A, *Phys Rev Lett*, 112 (2014) 172501.
13 Oganessian Y T, Utyonkov V K, Lobanov Y V, Abdullin F S, Polyakov A N & Sagaidak R N, *Phys Rev C*, 79 (2009) 024603.
14 Düllmann C E, TASCA Collaboration, in: Fission and Properties of Neutron-Rich Nuclei, 44, World Scientific, Singapore, (2013) 271.
15 Hofmann S, Heinz S, Mann R, Maurer J, Münzenberg G M, Antalic S, Barth W, Burkhard H G & Dahl L, *Eur Phys J A*, 52 (2016) 116.
16 Zhu L, Xie W J & Zhang F S, *Phys Rev C*, 89 (2014) 024615.
17 Zu-Hua L & Jing-Dong B, *Phys Rev C*, 84 (2011) 031602(R).
18 Wang N, Zhao E G, Scheid W & Zhou S G, *Phys Rev C*, 85 (2012) 041601(R).
19 Lougheed R, Landrum J, Hulet E, Wild J, Dougan R, Dougan A, Gäggeler H, Schädel M & Moody K, *Phys Rev C*, 32 (1985) 1760.
20 Nasirov A K, Giardina G, Mandaglio G, Manganaro M, Hanappe F, Heinz S, Hofmann S, Muminov A I & Scheid W, *Phys Rev C*, 79 (2009) 024606.
21 Adamian G, Antonenko N & Scheid W, *Eur Phys J A*, 41 (2009) 235.
22 Manjunatha H C & Sridhar K N, *Eur Phys J A*, 53 (2017) 97.
23 Manjunatha H C & Sridhar K N, *Eur Phys J A*, 53 (2017) 196.
24 Manjunatha H C & Sridhar K N, *Nucl Phys A*, 962 (2017) 7.
25 Manjunatha H C & Sowmya N, *Nucl Phys A*, 969 (2018) 68.
26 Manjunatha H C, *Int J Mod Phys E*, 25 (2016) 1650100.
27 Manjunatha H C, *Int J Mod Phy E*, 25 (2016) 1650074.
28 Manjunatha H C, *Nucl Phy A*, 945 (2016) 42.
29 Manjunatha H C, Chandrika B M & Seenappa L, *Mod Phys Lett A*, 31 (2016) 1650162.
30 Manjunatha H C & Sridhar K N, *Nucl Phys A*, 975 (2018) 136.
31 Manjunatha H C & Sowmya N, *Pramana J Phys*, 90 (2018) 62.
32 Manjunatha H C, *Indian J Phys*, 92 (2018) 507.
33 Manjunatha H C, *Nucl Phys A*, 971 (2018) 83.
34 Manjunatha H C & Sowmya N, *J Radiat Nucl Chem*, 314 (2017) 991.
35 Manjunatha H C & Sridhar K N, *Eur Phys J A*, 53 (2017) 156.
36 Blocki J, Randrup J, Swiatecki W J & Tsang C F, *Ann Phys*,105 (1977) 427.
37 Myers W D & Swiatecki W J, *Phys Rev C*, 62 (2000) 044610.
38 Wong C Y, *Phys Lett B*, 42 (1972) 186.
39 Zagrebaev V, Greiner W, *Phys Rev C*, 78 (2008) 034610.
40 Ignatyuk A V, (1985) IAEA report INDC(CCP)-233/L.
41 Kramers H A, *Physica*, 7 (1940) 284.
42 Sierk A J, *Phys Rev C*, 33 (1986) 2039.